Global NEST Journal, Vol 22, No 2, pp 369-380

Optimization of photocatalytic degradation of naproxen from aqueous solutions with UV/ZnO process: response surface methodology (RSM)

Karimi P.[1] and Malakootian M.[1,2]*

[1]Environmental Health Engineering Research Center, Kerman University of Medical Sciences, Kerman, Iran

[2]Department of Environmental Health, School of Public Health, Kerman University of Medical Sciences, Kerman, Iran

Received: 29/07/2018, Accepted: 24/09/2020, Available online: 13/10/2020

*to whom all correspondence should be addressed: e-mail: m.malakootian@yahoo.com, m_malakootian@kmu.ac.ir

https://doi.org/10.30955/gnj.002841

Graphical abstract

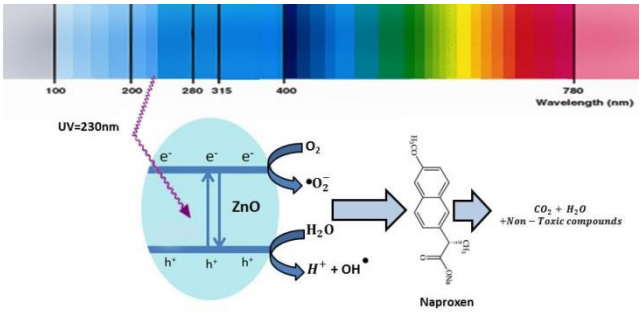

Abstract

The aim of this study was to optimize the removal of Naproxen (NPX) by the UV/ZnO photocatalytic process using response surface methodology based on Central Composite Design (CCD). The effect of parameters such as ZnO concentration, contact time, pH, temperature, and initial NPX concentration were studied. The ANOVA results indicated high coefficient values of adjusted R^2 (0.9843) and predicted R^2 (0.9695). The quadratic model with the highest R-squared designation was chosen to predict the NPX removal efficiency of the UV/ZnO process. Under optimal conditions that include an optimum initial NPX concentration of 21.59 mg/L, ZnO concentration of 371.15 mg/L, contact time of 73.92 min, pH of 6.87, and temperature of 24.35°C, a NPX removal efficiency value of 71.19% was obtained. The results show that the removal of NPX is most affected by the variables- initial NPX concentration, time, pH, and ZnO concentration, respectively, but temperature as a variable does not have a significant effect on the efficiency of the process. Moreover, the NPX photodegradation kinetics can be explained through the pseudo-first-order model. The UV/ZnO photocatalytic method has high potential for the removal of NPX, and that CCD is an appropriate method to optimize the operating conditions for NPX photodegradation.

Keywords: Central composite design, naproxen, photocatalytic process, degradation, aqueous solutions, UV/ZnO.

1. Introduction

The increased spread of diseases has led to a significant rise in the use of chemical drugs. The remnants of these drugs, after metabolism in the bod, along with their metabolites are excreted in the urine and stools and are released via wastewater into the environment (Hoseini *et al.*, 2015). In addition, wastewater also receives drug and chemical effluents from hospitals and chemical industries. These drug compounds are not completely eliminated in the treatment process of sewage plants and subsequently, lead to environmental contamination, Wastewater treatment plants are known as one of the most significant pathways for transfer of disposable drugs into the environment. The presences of microbial agents in aquatic environments are a serious threat to the ecosystem due to biological imbalances and bacterial resistance (Rahmani *et al.*, 2015). The most commonly used drugs are non-steroidal anti-inflammatory drugs (NSAIDs) that are found in trace amounts in drinking water. Naproxen (NPX) is one of the most frequently used NSAIDs in the treatment of musculoskeletal pain and rheumatoid arthritis. This drug, as an aromatic and propionic acid derivative, is extensively detected in surface water, groundwater, and influents from the pharmaceutical industry, and has hazardous effects on the aquatic environments (Carballa *et al.*, 2004). Various methods have been used to remove drug compounds from aqueous solutions. These include adsorption (Malakootian *et al.*, 2018; Malakootian *et al.*, 2019a) membrane processes (reverse osmosis), ultrasonic removal, and advanced oxidation processes, such as ozonation, photo-Fenton (Sun *et al.*, 2009) peroxidation with UV radiation, hybrid advanced oxidation process (Klavarioti *et al.*, 2009), and photodegradation (Devi *et al.*, 2013; Gad-Allah *et al.*, 2011; Malakootian *et al.*, 2019b; Malakootian *et al.*, 2020; Nasiri *et al.*, 2019; Tamaddon *et al.*, 2020a; Tamaddon *et al.*, 2020a).

Among these methods, the advanced oxidation process with photocatalytic methods are considered economical and effective as well as an environmentally compatible technology associated with sustainable wastewater treatment (Malakootian *et al.*, 2015; Seid-Mohammadi *et al.*, 2016)

The use of these methods, in combination with ultraviolet light and semiconductors such as ZnO, NiO, WO_2, and TiO_2, are of particular importance in solving environmental and global energy problems (Chen *et al.*, 2010; Liu *et al.*, 2014).The ZnO conductive layer acts as a photocatalyst due to high photosensitivity, surface-to-volume ratio, and stability along with its non-chemical nature; the wide energy gap and higher efficiency in the production of hydroxyl radicals have attracted particular attention. This energy gap of the ZnO nanoparticle attracts a large portion of UV light (Nagajyothi *et al.*, 2014; Rezaee *et al.*, 2012). The other special properties of ZnO nanoparticles include electromechanical coupling coefficient and high catalytic activity, adsorption of ultraviolet light, and anti-bacterial properties (Abbasian *et al.*, 2012). One of the most important features to be considered in the operational and pre-design scale of using any method in wastewater treatment is the selection of optimal process conditions. The proposed method should create minimal impact in terms of environmental pollution as well as be cost effective. There are several ways to optimize the effective parameters in processes, one of which is the response surface methodology (RSM). This method is used when the response to the problem (target) is influenced by several independent variables (inputs) and the goal is to optimize these responses (Im *et al.*, 2014).

The RSM method can be based on various designs such as CCD, BOX-Behnken, one factor, D-optimal, etc. However, of these, the central composite design (CCD) is considered very useful (Khataee *et al.*, 2010). An important advantage of this statistical method is that it uses the conditions of response level to determine the optimal conditions, thus allowing the expression of each independent variable's impact. Various studies have been conducted on the removal of NPX from aqueous solutions (Karaca *et al.*, 2016). However, research using the CCD method to optimize the UV/ZnO photocatalytic process has not been reported. The purpose of the research is to design and optimize the photocatalytic process of UV/ZnO in the removal of NPX from aqueous solutions using the CCD method.

2. Materials and methods

The experimental study was conducted at the Environmental Health Engineering Research Center of Kerman University of Medical Sciences in 2018.

2.1. Photoreactor preparation

The photocatalytic process was run in a Plexiglas 500 mL reactor dimensioning (10x10x8) cm. The photoreactor was mixed using a peristaltic pump (Cole-Parmer, Vernon Hills, IL, USA) and a magnetic stirrer at 200 rpm. A total of three Phillips UV lamps (6 W) were placed on the reactor. The three Phillips lamps UV-C (6 W, 3600µw/cm2) was used as a UV-light source. (wavelength) UV-C lamp with a peak intensity of 254 nm (Philips, The Netherlands). The external surface of the reactor was covered with aluminum foil for UV safety and energy consideration. The schematic of the reactor is shown in Figure 1.

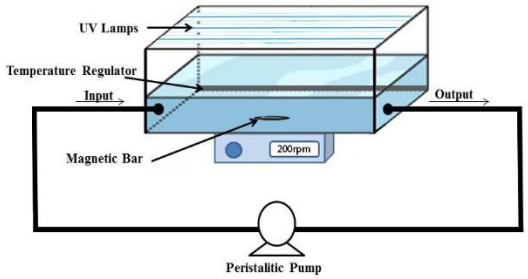

Figure 1. Schematic of the photoreactor used in the NPX photocatalytic degradation process

An aqueous solution of NPX was prepared by adding an appropriate amount of NPX to ethanol to yield 1000 mg/L stock solution. The photoreactor is filled with NPX of different concentrations with volume 300 mL. The pH solution was adjusted by adding sulfuric acid and sodium hydroxide 0.1 N. After the reaction, the samples (at specified intervals) were centrifuged at 4000 rpm for 10 minutes and filtered through a 0.45 µm membrane filter. To detect the adsorption and desorption between the NPX and photocatalyst, the NPX solution was placed in the dark for 30 minutes before exposure to the UV lamp.

The variable conditions such as initial concentration of NPX (10, 21.59, 30, 38.41, 50 mg/L), ZnO concentration (100, 244.8, 455.11, 600 mg/L), irradiation time (10, 36.08, 73.92, 100 min), pH (5, 6.73, 9.26, 11), and temperature (20, 24.35, 30.65, 35 °C) were applied to determine the amount of decomposition and extent of removal possible; accordingly, the optimal amount for each of these variables was recorded. The initial and final concentrations of NPX in the synthetic solutions were determined by a UV/Vis spectrophotometer (Shimadzu UV-1800 model at 230 nm). The pH of the solution was measured by a pH meter (Hanna Instruments, Japan) and the temperature was set by the Atman 100W Aquamarine heater AT180.

NPX with a purity of 99% was obtained from a pharmaceutical drug company (Drugstore Pharmacy, Tehran, Iran). The ZnO nanoparticles with 99.8% purity, average particle size of 60–72 nm, and a specific surface area of 15–25 m^2/g was obtained from Sigma-Aldrich, USA. Distilled water was used to prepare the synthetic solutions. The efficiency of NPX removal was calculated using Eq. 1.

$$R = \frac{(C_0 - C_t)}{C_0} \times 100 \quad (1)$$

Where R is the removal efficiency (%); C_0 and C_t are the initial and equilibrium concentration of NPX (mg/L), respectively.

The experiments were performed using techniques set forth in the standard methods for the examination of water

and wastewater (20th Edition.). The kinetics of NPX degradation were also determined. The CCD method was used for designing the experiments, as well as optimizing and analyzing the results using Design-Expert 7 software.

2.2. Experimental design based on CCD

Using the CCD method in the experimental design helped investigate the effect of independent variables on the response variable (process efficiency in NPX removal) as well as determine the optimal conditions (Table 1).

Based on the CCD matrix, 50 experiments were conducted to evaluate the effect of different variables with ZnO concentration (100–600 mg/L), time (10–100 min), pH (5–11), temperature (20–35°C), and initial NPX concentration (10–50 mg/L). The results have been analyzed by determining the coefficient R^2, ANOVA, and statistical response curves, which were then compared with the linear, two factor (2F), and quadratic models. The p-value<0.05 was considered as a significant level. The optimum conditions were performed by statistical analysis in order to obtain optimal points of each parameter and the best mathematical equation corresponding to the model.

3. Results and discussion

3.1. Investigation of adsorption-desorption

Since the adsorption of heterogeneous processes plays an important role in the evaluation of photocatalytic degradation, this process was performed separately before the design stage. The results of low removal efficiency (NPX) (< 3%) were shown by the adsorption process with ZnO at different concentrations and conditions (Méndez-Arriaga, Gimenez, etal., 2008) (Figure 2).

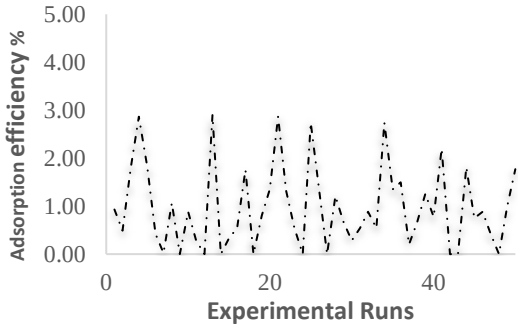

Figure 2. Investigate the adsorption in different experiments

3.1.1. Investigating the efficiency of NPX removal by UV, ZnO, and UV/ZnO

In order to investigate the effect of operational parameters on the process efficiency of NPX removal, the roles of adsorption, photolysis, and photocatalysis were determined separately. For this purpose, the effect of UV, ZnO, and UV/ZnO atvariables: NPX=21.59 mg/L, pH=9.26, temperature=30.65°C, ZnO=455.11 mg/L, and time = 36.07 minutes were investigated (Figure 3).

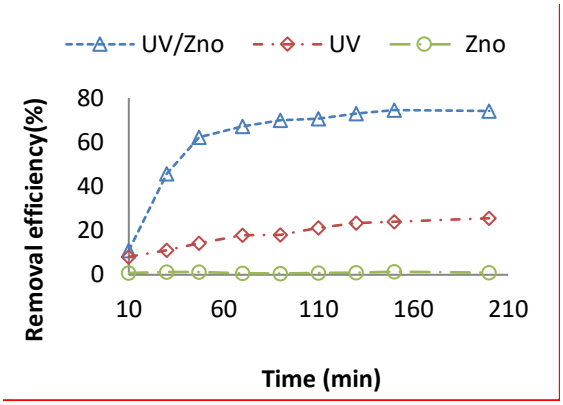

Figure 3. Removal efficiency of different processes involved in adsorption, photolysis and photocatalytic degradation Of NPX (pH=9.26, Temperature=30.65 °C, ZnO concentration=455.11 mg/L and NPX=21.59 mg/L)

The efficiency of UV radiation during the photolysis process was less than 30%, clearly indicating the need for an exhaling factor in the photocatalytic processes. In the UV/ZnO combination process, due to photocatalytic reactions and the emergence of free active radicals, a significant increase in process efficiency was observed.

Table1. Independent process variables, range and levels used for CCD design

Independent variables	Factors	-1	0	+1
Naproxen (mg/L)	A	10	30	50
ZnO (mg/L)	B	100	350	600
Time (min)	C	10	55	100
pH	D	5	8	11
Temperature (°C)	E	20	27.5	35

3.2. XRD analysis

X-ray diffraction (XRD) was used to study the crystalline and wurtzite structure of ZnO nanoparticles as is shown in the XRD pattern in (Figure 4).

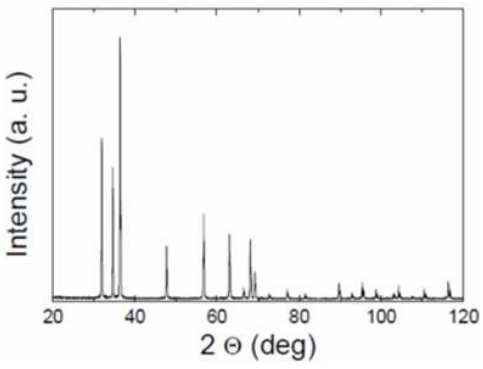

Figure 4. XRD pattern of ZnO nanoparticle

The nanoscale X-ray diffraction patterns showed high-intensity multi-courier particles at low angles (2θ=30°– 35°). Apart from these, there were several poor couriers at higher angles (2θ=50°–60°). The x-ray diffraction peaks in

the XRD analysis represent the hexagonal structure of the ZnO crystal, which confirms its purity.

Table 2. Experimental and predicted values of NPX photodegradation

Run	Naproxen (mg/L)	ZnO concentration (mg/L)	Reaction time (min)	pH	Temperatures (°C)	Removal rate (%)	Predicted (%)
1	21.59	455.11	36.08	9.26	30.65	61.97	61.60
2	38.41	244.89	36.08	9.26	24.35	45.05	46.27
3	21.59	455.11	73.92	6.74	30.65	62.05	63.04
4	30	350	55	11	27.50	55.11	53.24
5	30	350	55	8	27.50	68.93	67.79
6	21.59	455.11	36.08	6.74	24.35	60.27	59.42
7	38.41	455.11	36.08	9.26	30.65	64.44	64.12
8	38.41	244.89	36.08	9.26	30.65	59.57	61.28
9	30	350	55	8	27.50	48.29	47.53
10	21.59	455.11	36.08	6.74	30.65	23.19	21.88
11	38.41	455.11	36.08	6.74	30.65	55.43	54.38
12	30	350	100	8	27.50	33.46	34.25
13	30	350	55	5	27.50	69.03	70.12
14	30	350	55	8	27.50	52.23	51.43
15	30	350	55	8	20	71	71.86
16	38.41	244.89	73.92	9.26	30.65	60	58.70
17	50	350	55	8	27.50	63.67	63.16
18	30	350	10	8	27.50	51.15	51.25
19	38.41	244.89	36.08	6.74	30.65	58.50	60.13
20	21.59	244.89	73.92	9.26	30.65	55.74	53.93
21	30	350	55	8	27.50	61.23	61.85
22	38.41	455.11	73.92	9.26	30.65	56.98	56.90
23	38.41	455.11	73.92	6.74	30.65	53.76	53.90
24	30	350	55	8	35	53.40	54.48
25	21.59	455.11	36.08	9.26	24.35	55.97	55.07
26	21.59	244.89	36.08	6.74	30.65	33.04	32.83
27	30	350	55	8	27.50	57.34	57.62
28	21.59	455.11	73.92	6.74	24.35	40.06	40.92
29	38.41	455.11	36.08	6.74	24.35	69.28	70.17
30	38.41	455.11	36.08	9.26	24.35	55.75	54.89
31	38.41	244.89	73.92	6.74	24.35	68.66	67.62
32	21.59	244.89	36.08	9.26	30.65	57.39	57.87
33	38.41	455.11	73.92	9.26	24.35	67.12	66.60
34	21.59	455.11	73.92	9.26	30.65	35.86	36.78
35	21.59	455.11	73.92	9.26	24.35	51.22	52.58
36	10	350	55	8	27.50	58.78	57.83
37	38.41	244.89	73.92	9.26	24.35	34.16	35.04
38	21.59	244.89	36.08	9.26	24.35	63.03	62.56
39	21.59	244.89	3.92	6.74	30.65	69.35	68.78
40	38.41	244.89	36.08	6.74	24.35	55.12	56.09
41	30	600	55	8	27.50	56.22	57.26
42	30	350	55	8	27.50	58.76	58.13
43	30	350	55	8	27.50	59.36	59.03
44	21.59	244.89	73.92	6.74	24.35	57.72	59.03
45	38.41	455.11	73.92	6.74	24.35	59.40	59.03
46	21.59	244.89	36.08	6.74	24.35	60	59.03
47	21.59	244.89	73.92	9.26	24.35	58.32	59.03
48	30	100	55	8	27.50	57.35	59.03
49	30	350	55	8	27.50	60	59.03
50	38.41	244.89	73.92	6.74	30.65	59.82	59.03

3.3. Design and analysis by CCD method

The CCD method is a powerful tool in empirical modeling of the relationships between experimental and predicted model results (Swamy *et al.*, 2014). A total of five variables (initial NPX concentration, pH, time, temperature, and photocatalyst concentration) were investigated at three levels. The NPX removal efficiency was considered the dependent variable (response). All the experiments were performed under designed and optimal conditions, and the effect of each variable on the NPX removal efficiency was recorded.

3.4. Fitting model

The design matrix of the experimental values predicted by the CCD model is reported in Table 2.

Table 3. Results of model adequacy tested in the CCD design

Source	Sum of Squares	Df	Mean Square	F Value	p-value Prob> F	Adjusted R-Squared	Predicted R-Squared	Remarks
Linear	1612.52	37	43.58	39.19	< 0.0001	0.6458	0.5799	
2FI	348.64	27	12.91	11.61	0.0001	0.9000	0.8953	
Quadratic	39.97	22	1.82	1.63	0.2601	0.9843	0.9695	Suggested
Cubic	8.13	7	1.16	1.04	0.4780	0.9892	0.9429	Aliased
Pure Error	7.79	7	1.11	-	-			

The quadratic model with the highest R-squared designation was chosen to predict NPX removal efficiency in the UV/ZnO process

Table 4. ANOVA results of response surface quadratic model for photodegradation of NPX using UV/ZnO

Source	Sum of squares	df	Mean square	F_{value}	P-value	Status
Model	5086.50	20	254.32	154.44	< 0.0001	Significant
A-Naproxen	1701.94	1	1701.94	1033.50	<0.0001	Significant
B-ZnO	52.83	1	52.83	32.08	<0.0001	Significant
C-Time	1449.49	1	1449.49	880.20	< 0.0001	Significant
D-pH	308.23	1	308.23	187.17	<0.0001	significant
E-Temperatures	1.46	1	1.46	0.88	0.3548	Not Significant
AB	61.22	1	61.22	37.17	< 0.0001	significant
AC	96.88	1	96.88	58.83	< 0.0001	Significant
AD	213.21	1	213.21	129.47	< 0.0001	Significant
AE	23.39	1	23.39	14.21	0.0007	Significant
BC	52.12	1	52.12	31.65	< 0.0001	Significant
BD	58.43	1	58.43	35.48	< 0.0001	Significant
BE	36.81	1	36.81	22.35	< 0.0001	Significant
CD	538.08	1	538.08	326.75	< 0.0001	Significant
CE	112.28	1	112.28	68.18	< 0.0001	Significant
DE	71.46	1	71.46	43.39	< 0.0001	Significant
A^2	93.48	1	93.48	56.77	< 0.0001	Significant
B^2	25.37	1	25.37	15.40	0.0005	Significant
C^2	181.81	1	181.81	110.40	< 0.0001	Significant
D^2	20.17	1	20.17	12.25	0.0015	Significant
E^2	3.10	1	3.10	1.89	0.1803	Not Significant
Residual	47.76	29	1.65	-	-	-
Lack of fit	39.97	22	1.82	1.63	0.2601	Not Significant
Pure Error	7.79	7	1.11	-	-	-
Core total	5134.25	49	-	-	-	-

In Figure 5, the correlation between the real and predicted values of the model is presented.

The points given in this plan are relatively close to the straight line and give satisfactory correlations. Figure 6 shows the normalization of data.

The results showed that the responses obtained from the experiments are close to the straight line and represent the normal distribution of the data.

3.5. Model Selection

To select a model and regression equations for the process, two factor (2F), quadratic, and cubic models were investigated in order to predict the results with proper power of the linear models. The matching of each model was examined (Table 3).

3.6. Model Assessment

In order to evaluate the selected model and its significant test, ANOVA analysis was used, the results using the UV/ZnO process are shown in Table 4.

According to the analysis, the F-values of initial NPX concentration, time, pH, and ZnO concentration are the most important variables affecting process efficiency, whereas temperature, with the lowest value of F-value and p-value > 0.05, does not have a significant effect on process efficiency.

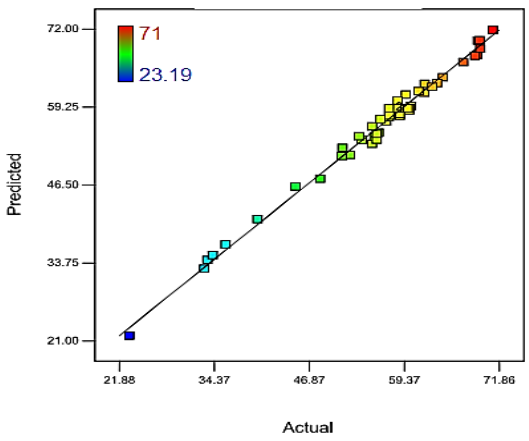

Figure 5. Comparison between predicted and experimental values of NPX photodegradation

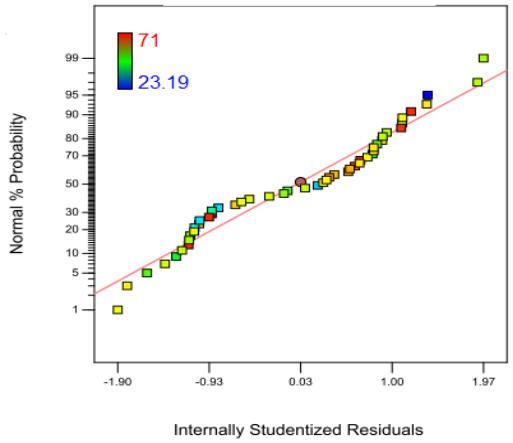

Figure 6. Normal probability plots of studentized residuals

Factors with a p-value <0.05 were considered significant and remained in the model. Accordingly, Eq. 2 shows the proposed model:

$$Y=59.03 - 6.27A + 1.10B+5.78C - 2.67D + 1.38AB + 1.74AC - 2.58AD + 0.85AE - 1.28BC + 1.35BD - 1.07BE + 4.10CD - 1.87CE + 1.49DE - 1.30A^2 - 0.68B^2 - 1.81C^2 + 0.6D^2 \quad (2)$$

Where Y is the percentage of NPX removal and codes A, B, C, D, and E are NPX initial concentration, ZnO, time, pH, and temperature, respectively.

3.7. Model validation

The results of validation and correlation coefficients of the model are presented in Table 5.

The statistical parameters selected for fitting the model are the mean, standard deviation, and coefficient of variation, indicating the status of data deletion in the response. As seen, the coefficient of variation is 2.29% and indicates the accuracy of measurement and reliability of the tests.

PRESS is the proportion of the model in each of the points so that the lower the better. Predicted R-Squared is an error value, used to evaluate the quality of the proposed model. The explained sum of squares is described by the total squares, and the numerical value varies between zero–1. The closer the number is to one, the higher the validity of the proposed model (Shokohi *et al.*, 2017). The value of R-squared in this study is equal to 0.99 and shows the strength and high adaptability of the proposed model for the removal of NPX by the UV/ZnO photocatalytic process (Aghel *et al.*, 2017).

Table 5. The correlation coefficients for response surface quadratic model

Parameter	Value	Parameter	Value
Standard deviation	1.28	R-Squared	0.9907
Mean	56.07	Adjusted R-Squared	0.9843
C.V.%	2.29	Predicted R-Squared	0.9695
PRESS	156.53	Adeq Precision	60.101

3.8. Optimum Model Conditions

In order to achieve the optimum conditions for removal of NPX, the UV/ZnO photocatalytic process used the Derringer utility function. In this method, the process performance is expressed by a number between zero and one, in which the 'zero' indicates an undesirable response and the 'one' represents the desirable response (Awotwe-Otoo *et al.*, 2012). The results are shown in Figure 7.

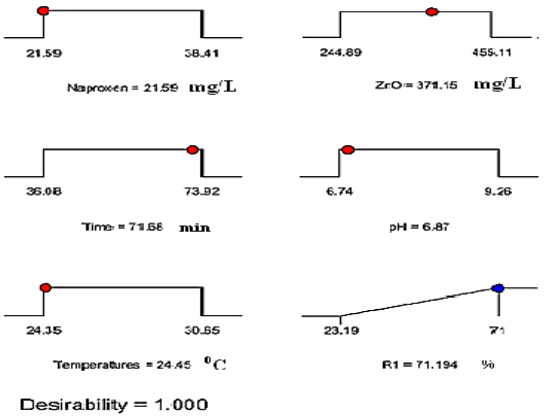

Figure 7. Desirability ramp for NPX photodegradation process optimization

The best model for prediction included input conditions: initial NPX concentration of 21.59 mg/L, ZnO concentration of 371.15 mg/L, time of 73.92 min, pH of 6.87, and temperature of 24.35 °C. The proposed efficiency of the model and the actual efficiency resulting from the photocatalytic reaction in optimal conditions were 69.45% and 71.19%, respectively, indicating a strong correlation between model prediction and actual conditions.

3.9. Effect of initial NPX concentration

The results regarding the effects of NPX concentration with increasing contact time on NPX removal efficiency are shown in Figure 8.

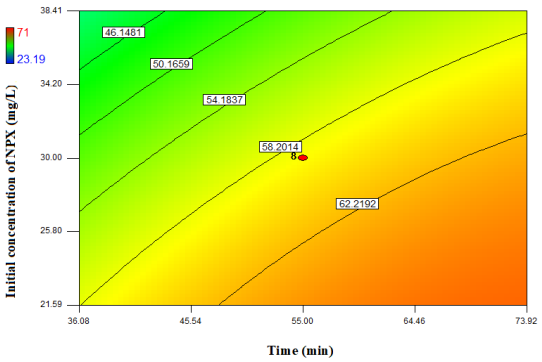

Figure 8. Effect of initial concentration of NPX at different times on removal efficiency

With increase in contact time and initial concentration amounts of NPX, the removal efficiency was reduced. At high concentrations of NPX, more time was taken in the process to achieve significant removal efficiency. The reduction in removal efficiency caused by the increase in initial concentration may be due to the limited number of active hydroxylation ion production sites available for NPX degradation at high concentrations and low times. In other words, to achieve optimum efficiency in the photocatalytic process, a balance between the production of hydroxyl ions and the initial concentration of NPX is necessary; hence, increasing the initial concentration of NPX can significantly reduce the process efficiency (Darvishi *et al.*, 2015; Méndez-Arriaga *et al.*, 2008).

3.10. The effect of reaction time

The effect of contact time on NPX removal rate was investigated within a specific time interval (10–100 minutes). Results are shown in Figure 9.

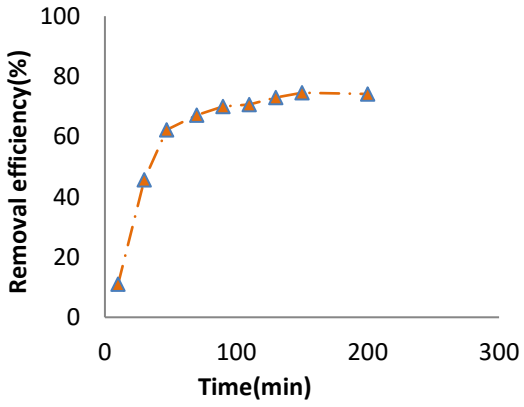

Figure 9. The effect of contact time on NPX removal efficiency (Experimental condition: NPX Concentration: 21.59 mg/L, ZnO Concentration: 371.15 mg/L, pH=6.87, temperature=24.45oC)

By increasing the irradiation time from 10 to 70 minutes, the removal efficiency increased. This could be attributed to an increase in the exposure time of the target with the stimulated catalyst (Darvishi *et al.*, 2016). The statistical analysis also showed a significant correlation between these two parameters (p-value <0.0001). However, with a further increase of up to 90 minutes, no significant effect was observed on the removal efficiency. The high NPX removal efficiency in the initial 70 minutes can be attributed to the rapid degradation of NPX by free radicals produced by the electron excitation of ZnO nanoparticles. With the increase in reaction time, although the ZnO excitation process and the production of free radicals did not diminish, the degradation process of NPX produced intermediate compounds which required the available free radicals to degrade these compounds too, and thus the reduction rate decreased at reaction time greater than 70 minutes (Fu *et al.*, 2011).

3.11. Effect of photocatalyst concentration

The effect of varying concentrations of ZnO nanoparticles on the efficiency of the removal process is shown in Figure 10a.

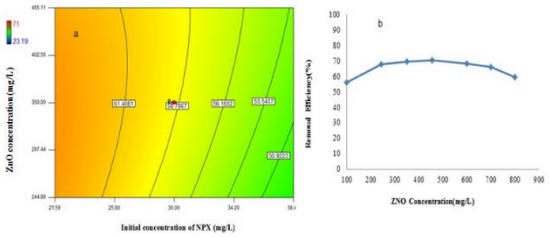

Figure 10. (a) The relation of ZnO concentration with NPX initial concentration, (b) The relation of ZnO concentration with NPX removal efficiency

According to the results of Figure 10a, increasing the concentration of ZnO nanoparticles caused the efficiency of the process to increase too. This could be attributed to the increase in active levels of the catalyst, and consequently, to the enhanced production of hydroxyl and superoxide radicals. The statistical analysis also showed that the concentration ratio of ZnO nanoparticles is statistically significant (p-value = <0.0001). The ZnO concentration increased the process efficiency only to a certain extent; any further increase in the ZnO concentration had no effect on the retrieval efficiency (Figure 10b). On the contrary, an excessive increase in the ZnO nanoparticle concentration resulted in increased opacity,
reduced UV light penetration, increased photoconductive pathways, and decreased total surface area, ultimately causing a negative effect on removal efficiency (Ahmadimoghadam *et al.*, 2016; Gharaghania and Malakootiana, 2017; Maleki *et al.*, 2016).

It should be mentioned that photostability of ZnO decreases under prolonged light irradiation, due to photocorrosion mechanisms (Hamid *et al.*, 2017). According to Literature review, an anti-photocorrosion of ZnO is surface hybridization of ZnO with graphite-like carbon layers (Han *et al.*, 2014; Zhang *et al.*, 2009). It significantly suppresses the coalescence and crystal growth of ZnO nanoparticles during high-temperature treatment. In another study hybridization of ZnO with C3N4 led to an enhanced photoactivity (Wang *et al.*, 2011). Haiqing Yao *et al.* also reported reducing of the ZnO particle sizes to below

7 nm by synergetic effect can help to reduce photocorrosion of Zno (Yao *et al.*, 2016).

3.12. Effect of pH

The pH of a solution plays an important role in the photocatalytic degradation process. The effect of the initial pH of solution (in the range of 5–11) on the NPX removal efficiency is shown in Figure 11.

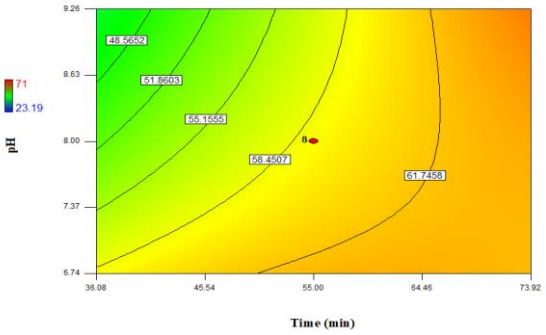

Figure 11. Effect of pH on process efficiency

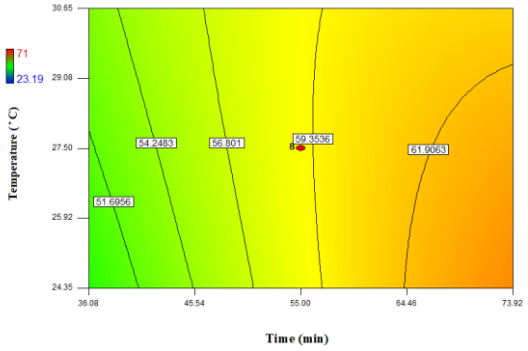

Figure 12. Effect of temperature on process efficiency (NPX=21.59 mg/L, ZnO=371.15 mg/L, Time=71.68 min, pH=6.87)

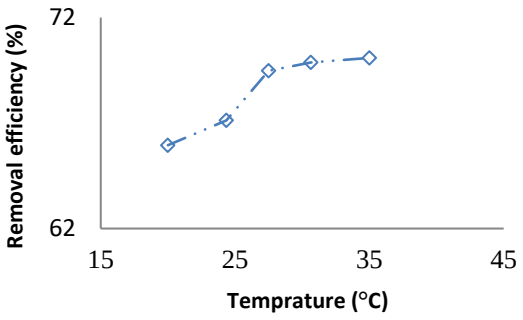

Figure 13. The removal efficiency of naproxen at various temperatures NPX=21.59 mg/L, ZnO=371.15 mg/L, Time=71.68 min, pH=6.87)

The process efficiency was highest at pH levels below 7, so that in acidic pH conditions, the removal rate was higher than 55% at all times. Under periods of 50 minutes, the pH has a significant influence on process efficiency, such that by increasing the pH level the removal efficiency decreased. With an increase in time, the influence of pH value decreases resulting in improved removal efficiency. The process removal efficiency changed by the chemical nature of the ZnO nanoparticles. The point of zero charge of ZnO is pH = 9 (Rastkari *et al.*, 2017). Therefore, when the pH of the solution is less than 9 and more than NPX pK_a (pK_a = 4.2), the NPX species which are anions and the ZnO adsorb to the positive charge, causing the removal efficiency to increase. At pH values above pH_{pzc}, the ZnO level has a negative charge, which results in the removal of electro-static NPX from ZnO levels, reducing adsorption, and finally reducing the efficiency of removal (Darvishi *et al.*, 2015; Méndez-Arriaga *et al.*, 2008; Zhang *et al.*, 2015).

At high pH levels, OH radicals become $O_2^{\bullet -}$ and $O_2H^{\bullet}$, which have a lower degrading activity than $OH^{\bullet}$. Thus, the efficiency of NPX degradation is reduced at high pH levels (Torki,and Faghihian, 2018).

$$OH^{\bullet} + HO^{-}_2 \rightarrow H_2O + O^{\bullet -}_2 \quad (3)$$

$$OH^{\bullet} + H_2O_2 \rightarrow H_2O + O_2H^{\bullet} \quad (4)$$

3.13. Effect of temperature

In order to investigate the effect of temperature on the photocatalytic degradation of NPX in aqueous solutions, the changes in removal rate at a temperature range of 20-35 °C were investigated. The results are shown in Figures 12 and 13.

The photocatalytic processes are not primarily dependent on temperature (Barka *et al.*, 2010). Although NPX removal efficiency is directly related to temperature, there was no significant effect in terms of the temperature range. This is because the production of free radicals does not depend on temperature. The statistical analysis also shows that there is no significant relationship between temperature and process efficiency. (P-value = 0.3548).

3.14. Reaction kinetics

The common kinetics used in the photocatalytic processes for the degradation of organic matter is of the pseudo-first-order type (Kanakaraju *et al.*, 2015; Turki *et al.*, 2015). Therefore, after determining the optimal conditions, the first-order kinetics was investigated. Eq. 5 shows the linear first-order kinetic:

$$\ln\left(\frac{C_0}{C_t}\right) = k_{obs}t \quad (5)$$

Where C_0 is the initial concentration (mg/L) of NPX, C_t is concentration (mg/L) at time, t (min), and K_{obs} is constant reaction rate (min^{-1}). The parameters of the pseudo-first model of NPX removal in the vicinity of the ZnO photocatalyst are shown in Table 6.

Table 6. Pseudo-First-Order kinetic parameters of NPX (21.59 mg/L) photodegradation (pH=6.87, Temperature=24.35 °C)

NPX (mg/L)	R^2	k_{obs}(1/min)	1/ k_{obs}(min)
21.59	0.9901	0.0143	69.93
30	0.9873	0.0126	79.36
38.41	0.9863	0.0085	117.65

As shown, the reaction constant decreased when the concentration of NPX increased from 0.0143 to 0.0085. This shows that the rate of photocatalytic reaction, as seen in other studies, is due to the concentration of pollutants, the number of active catalytic active sites, and the transfer of NPX from the liquid phase to the ZnO surface (Ghaneian *et al.*, 2010; Turki *et al.*, 2015). The difference in reaction speed constants at various concentrations may also be due to either the various photocatalytic degradation mechanisms or the competition between degradation of the reactant and intermediate products (Massoudinejad *et al.*, 2016).

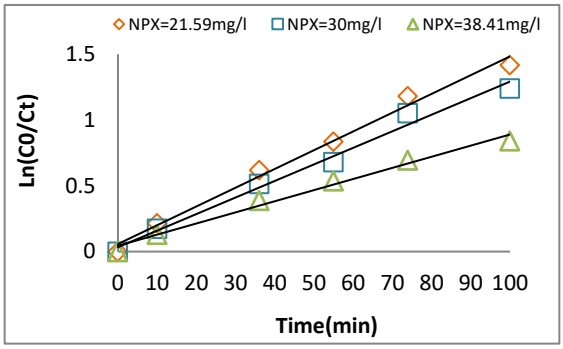

Figure 14. Linear Chart of the Pseudo-First-order Kinetic Model at Different Concentrations of the NPX

Figure 14 shows the linear diagram of the quasi-first-order kinetic model at different concentrations of NPX at different times.

Given the high R^2, there is a strong linear relationship between the variations of NPX concentration and exposure times, which confirms the utility of the pseudo-first-order model in describing changes in reaction speed and NPX removal rates at different times.

Result comparison between various studies and the present study for the removal of NPX

The comparison of results show that the efficiency of photocatalytic processes strongly depends on the reaction and the highest removal rate occurred in most studies over a period of 90 minutes. Upper times at operational scales have dramatically increased the dimensions of treatment processes, problem utilization, high cost design, and manufacturing processes (Zheng *et al.*, 2014). Most studies reported the highest NPX elimination efficiency at pH values <5, but as the pH values differ in most wastewater and water flows in the range of 6–9, pH values <6 also increase the cost of the consumption substance since it is a chemical (Massoudinejad *et al.*, 2016; Méndez-Arriaga *et al.*, 2008). Although TiO_2 treatment processes have shown a high efficiency in NPX removal, the use of these processes has been limited due to the tendency of TiO_2 particles to accumulate in the aqueous medium and create toxic interfaces (Jallouli *et al.*, 2016). Accordingly, the use of the UV/ZnO photocatalytic process can be considered a suitable option for the removal of NPX in aquatic environments and should be applied on an operational scale.

Table 7. Performance comparison of different photocatalyst process evaluated NPX removal

Methods	Temperature (°C)	Time (min)	pH	NPX removal (%)	Cons. catalyst	initial NPX concentration	References
Present study	24.45	71.68	6.87	71.19	Zno Cons.= 0.37g/L	21.59 mg/L	-
Ultra Sonic/ZnO/Montmorillonite	-	120	4.5	<80%	1.25 g/L+ 650 W/L US power	5mg/L	Méndez-Arriaga *et al.*, 2008
Nano-TiO_2 diatomite (NTD)	27	360	-	100	NTD=0.8g/l+UV intensity= 0.39 mw/cm^2	0.8 mg/L	Sun *et al.*, 2014
nitrogen and sulfur co-doped TiO_2 (N,S-TiO_2)	22±0.2	90	6	99.3	N,S-$TiO_{2=}$ 2.0 g /L+ solar irradiation (Xe lamp 300 W)	5mg/L	Eslami *et al.*, 2016
UV/TiO_2	24.85±1	180	6.5	83%	TiO_2=2 g /L + UV intensity= 11W	0.26 mmol/L	Jallouli *et al.*, 2016

3.15. Electrical energy efficiency

The Electrical Energy per Order (EEO) parameter Used for the first time in 1996 by Bolton *et al.* 1996 for advanced oxidation processes (Bolton *et al.*, 1996). EEO is the number of kilowatt hours of electrical energy required to reduce the concentration of NPX in water by 1 order of magnitude in a unit volume of NPX sample (kW m^{-3} order) according to flow equation:

$$E_{EO} = \frac{1000Pt}{60V} log \frac{C}{C_0}$$

where P =the input power (kW), t = the irradiation time (min), V = the volume of water (L), C and C0 = the final and initial and concentrations of NPX (Sharma *et al.*, 2016). Accordingly, The EEO values for degradation NPX by photocatalytic degradation of UV/ZnO process is 79.84 kWh m^{-3}. It shows that UV/ZnO process of *ZnO*

nanocatalyst has suitable energy efficiency for the photodegradation of NPX.

4. Conclusion

In summary, the UV/ZnO photocatalytic process has a high potential ability for degradation of NPX in aqueous solutions. According to ANOVA, the quadratic model with high predictive power has the ability to predict the results of the study (R^2 = 0.9907). Among the various variables examined, the most important parameters affecting system performance are NPX concentration > time> pH> ZnO concentration > temperature. The optimum conditions for removal of NPX are as follows: NPX = 21.59 mg/L, ZnO = 371.15 mg/L, time = 71.68 min, pH=6.87 and temperature=24.45◦C to give 71.19% removal efficiency. The examination and calculation of the process tradition showed the proper matching with the quasi-first-order model. (R^2> 0.98). It can be concluded that the UV/ZnO photocatalytic process is an appropriate option for high efficiency, low cost, and easy implementation for use in removal of NPX from aquatic solutions on an operational scale.

Acknowledgments

This research carried out in the Environmental Health Engineering Research Center at Kerman University of Medical Sciences and was sponsored by the Vice Chancellor for Research and Technology of the university. The authors take this opportunity to express their gratitude for the support and assistance extended by the facilitators during the course of this research.

References

Abbasian M., Yeghaneh F.S. and Khataee A. (2014), Synthesis of Polymethylstyrene/Zink Oxide (ZnO) Nanoparticles Nanocomposite by in situ*, Polymerization*, **12**(77), 44–52.

Aghel S., Bahramifar N. and Younesi H. (2017), Optimizing the Removal of Reactive Yellow 147 Using Magnetic photocatalyst Fe_3O_4@SiO_2@TiO_2 by Response Surface Methodology in Central Composite Design*, Journal of Mazandaran University of Medical Sciences,* **27**(149), 167–180.

Ahmadimoghadam M., Jaafarzadeh Haghighifard N., Mirali S., Jorfi S., Dinarvand F. and Alavi N. (2016), Efficiency Study on Nanophotocatalytic Degradation and Detoxification of CI direct blue 86 from Aquatic Solution Using UVA/TiO_2 and UVA/ZnO, *Journal of Mazandaran University of Medical Sciences,* **26**(143), 145–159.

Awotwe-Otoo D., Agarabi C., Faustino P.J., Habib M.J., Lee S., Khan M.A. and Shah R.B. (2012), Application of quality by design elements for the development and optimization of an analytical method for protamine sulfate, *Journal of Pharmaceutical and Biomedical Analysis,* **62**, 61–67.

Barka N., Qourzal S., Assabbane A., Nounah A. and Ait-Ichou Y. (2010), Photocatalytic degradation of an azo reactive dye, Reactive Yellow 84, in water using an industrial titanium dioxide coated media, *Arabian Journal of Chemistry,* **3**(4), 279–283.

Bolton J.R., Bircher K.G., Tumas W. andTolman C.A. (1996*),* Figures-of-merit for the technical development and application of advanced oxidation processes, *Journal of Advanced Oxidation Technologies,* **1**(1) ,13–17.

Carballa M., Omil F., Lema J.M., Ma L., García-Jares C., Rodríguez I., et al. (2004), Behavior of pharmaceuticals, cosmetics and hormones in a sewage treatment plant, *Water Research,* **38**(12), 2918–2926.

Chen Y., Lu C., Xu L., Ma Y., Hou W. and Zhu J.J. (2010), Single-crystalline orthorhombic molybdenum oxide nanobelts: synthesis and photocatalytic properties, *Cryst Eng Comm,* **12**(11), 3740–3747.

Darvishi Cheshmeh Soltani R., Rezaee A., Safari M., Khataee A.R. and Karimi B. (2015), Photocatalytic degradation of formaldehyde in aqueous solution using ZnO nanoparticles immobilized on glass plates, *Desalination and Water Treatment,* **53**(6), 1613–1620.

Darvishi C.S.R., Rezaee R., Hashemi H. and Safari M. (2016), Comparison of photocatalytic activity of synthesized and commercial Zno nanoparticels in dye removal in aqueous environment, *Health System Resaerch,* **12**(3), 278–283.

Devi L.G. and Kavitha R. (2013), A review on non metal ion doped titania for the photocatalytic degradation of organic *pollutants under UV/solar light: role of* photogenerated charge carrier dynamics in enhancing the activity, *Applied Catalysis B: Environmental,* **140**, 559–587.

Eslami A., Amini M.M., Yazdanbakhsh A.R., Mohseni-Bandpei A., Safari A.A. and Asadi A. (2016), N,S co-doped TiO2 nanoparticles and nanosheets in simulated solar light for photocatalytic degradation of non-steroidal anti-inflammatory drugs in water: a comparative study, *Journal of Chemical Technology and Biotechnology*, **91**(10), 2693–2704.

Fu M., Li Y., Lu P., Liu J. and Dong F. (2011), Sol–gel preparation and enhanced photocatalytic performance of Cu-doped ZnO nanoparticles, *Applied Surface Science,* **258**(4), 1587–1591.

Gad-Allah T.A., Ali M.E. and M.I. (2011) Badawy, Photocatalytic oxidation of ciprofloxacin under simulated sunlight, *Journal of Hazardous Materials*, **186**(1), 751–755.

Ghaneian M.T., Ehrampoush M.H., Ghanizadeh G.H., Dehvary M., Abootoraby M. and Jasemizad T. (2010), Application of solar irradiation/K2S2O8 photochemical oxidation process for the Removal of reactive blue 19 dye fromaqueous solutions, *Iranian Journal of Health and Environment,* **3**(2), 165–176.

Gharaghania M.A. and Malakootian M. (2017), Photocatalytic degradation of the antibiotic ciprofloxacin by ZnO nanoparticles immobilized on a glass plate, *Desalination and Water Treatment,* **89**, 304–314.

Hamid S.B.A., Teh S.J. and Lai C.W. (2017), Photocatalytic water oxidation on ZnO: a review, *Catalysts*, **7**(3), 93.

Han C., Yang M.Q., Weng B. and Xu Y.J. (2014), Improving the photocatalytic activity and anti-photocorrosion of semiconductor ZnO by coupling with versatile carbon, *Physical Chemistry Chemical Physics*, **16**(32), 16891–16903.

Hoseini M., Safari G.H., Kamani H., Jaafari J. and Mahvi A. (2015), Survey on Removal of Tetracycline Antibiotic from Aqueous Solutions by Nano-Sonochemical Process and Evaluation of the Influencing Parameters, *Iranian Journal of Health and Environment,* **8**(2), 141–152.

Im J.K., Yoon Y. and Zoh K.D. (2014*),* Optimization of naproxen and ibuprofen removal in photolysis using a Box–Behnken design: Effect of Fe (III), NO_3^-, and humic acid, *Journal of Environmental Science and Health, Part A,* **49**(4), 422–433.

Jallouli N., Elghniji K., Hentati O., Ribeiro A.R., Silva A.M. and Ksibi M. (2016), UV and solar photo-degradation of naproxen: TiO_2 catalyst effect, reaction kinetics, products identification and

toxicity assessment, *Journal of hazardous materials,* **304**, 329–336.

Kanakaraju D., Motti C.A., Glass B.D. and Oelgemöller M. (2015), TiO_2 photocatalysis of naproxen: effect of the water matrix, anions and diclofenac on degradation rates, *Chemosphere,* **139**, 579–588.

Karaca M., Kıranşan M., Karaca S., Khataee A. and Karimi A. (2016), Sonocatalytic removal of naproxen by synthesized zinc oxide nanoparticles on montmorillonite, *Ultrasonics Sonochemistry*, **31**, 250–256.

Khataee A.R., Zarei M. and Asl S.K. (2010), Photocatalytic treatment of a dye solution using immobilized TiO_2 nanoparticles combined with photoelectro-Fenton process: Optimization of operational parameters, *Journal of Electroanalytical Chemistry,* **648**(2), 143–150.

Klavarioti M., Mantzavinos D. and Kassinos D. (2009), Removal of residual pharmaceuticals from aqueous systems by advanced oxidation processes, *Environment International*, **35**(2), 402–417.

Liu T., Li B., Hao Y. and Yao Z. (2014), MoO_3-nanowire membrane and $Bi_2Mo_3O_{12}/MoO_3$ nano-heterostructural photocatalyst for wastewater treatment, *Chemical Engineering Journal,* **244**, 382–390.

Malakootian M., Yousefi N., Fatehizadeh A., Van Ginkel S.W., Ghorbani M., Rahimi S. and Ahmadian M. (2015). Nickel (II) removal from industrial plating effluent by fenton process, *Environmental Engineering and Management Journal,* **14**(4), 837–842.

Malakootian M., Hashemi M., Toolabi A. and Nasiri A. (2018). Investigation of nickel removal using poly(amidoamine) generation 4 dendrimer (PAMAM G4) from aqueous solutions, *Journal of Engineering Research,* **6**(2), 13–23.

Malakootian M., Nasiri A. and Mahdizadeh H. (2019a). Metronidazole adsorption on $CoFe_2O_4$/activated carbon@chitosan as a new magnetic biocomposite: Modelling, analysis, and optimization by response surface methodology, *Desalination and Water Treatment,* **164**, 215–227.

Malakootian M., Nasiri A., Asadipour A., Faraji M. and Kargar E. (2019b). A facile and green method for synthesis of $ZnFe_2O_4$@CMC as a new magnetic nanophotocatalyst for ciprofloxacin removal from aqueous media, *MethodsX,* **6**, 1575–1580.

Malakootian M., Khatami M., Mahdizadeh H., Nasiri A. and Amiri Gharaghani M. (2020). A study on the photocatalytic degradation of p-Nitroaniline on glass plates by Thermo-Immobilized ZnO nanoparticle, *Inorganic and Nano-Metal Chemistry,* **50**(3), 124–135.

Maleki A., Zandsalimi Y., Jafari M., Daraei H. and Sadeghi S. (2016), Photocatalytic Removal of Acid Red 18 Dye from Aqueous with ZnO Nanoparticles Synthesized by Hydrothermal Method, *Journal of Health*, **6**(5),498–506.

Massoudinejad M., Ghaderpoori M., Shahsavani A. and Amini M.M. (2016), Adsorption of fluoride over a metal organic framework Uio-66 functionalized with amine groups and optimization with response surface methodology, *Journal of Molecular Liquids,* **221**, 279–286.

Méndez-Arriaga F., Gimenez J. and Esplugas S. (2008), Photolysis and TiO2 photocatalytic treatment of naproxen: degradation, mineralization, intermediates and toxicity, *Journal of Advanced Oxidation Technologies.* **11**(3), 435–444.

Nagajyothi P.C., Sreekanth T.V.M., Tettey C.O., Jun Y.I. and Mook S.H. (2014), Characterization, antibacterial, antioxidant, and cytotoxic activities of ZnO nanoparticles using Coptidis Rhizoma, *Bioorganic & Medicinal Chemistry Letters,* **24**(17), 4298–4303.

Nasiri A., Tamaddon F., Mosslemin M.H. and Faraji M. (2019). A microwave assisted method to synthesize nano$CoFe_2O_4$@methyl cellulose as a novel metal-organic framework for antibiotic degradation, *MethodsX,* **6**, 1557–1563.

Rahmani K., Rahmani A., Rahmani H. and Zare M.R. (2015), Tetracycline Removal from Aqueous Solution by Nano Zero Valent Iron/UV/H_2O_2 Process, *Journal of Environmental Health Enginering,* **2(**4), 294–304.

Rastkari N., Eslami A., Nasseri S., Piroti E. and Asadi A. (2017), Optimizing Parameters on Nanophotocatalytic Degradation of Ibuprofen Using UVC/ZnO Processes by Response Surface Methodology, *Polish Journal of Environmental Studies,* **26**(2), 785–794.

Rezaee A., Masoumbeigi H., Soltani R.D.C., Khataee A.R. and Hashemiyan S. (2012), Photocatalytic decolorization of methylene blue using immobilized ZnO nanoparticles prepared by solution combustion method, *Desalination and Water Treatment,* **44**(1-3), 174–179.

Seid-Mohammadi A., Asgari G., Poormohammadi A., Ahmadian M. and Rezaeivahidian H. (2016), Removal of phenol at high concentrations using UV/Persulfate from saline wastewater, *Desalination and Water Treatment,* **57**(42), 19988–19995.

Sharma A.K., Tiwari R.K. and Gaur M.S. (2016), Nanophotocatalytic UV degradation system for organophosphorus pesticides in water samples and analysis by Kubista model, *Arabian Journal of Chemistry,* **9***,* 1755–1764.

Shokohi R., Shabanloo A. and Zamani F. (2017), Evaluation of efficiency of persulfate activated with heat in 2, 4-dinitrophenol degradation from aqueous solution by central composite design method, *Iranian Journal of Health and Environment,* **10**(2), 187–198.

Sun S-P., Guo H-Q., Ke Q., Sun J-H., Shi S-H., Zhang M-L., et al. (2009), Degradation of antibiotic ciprofloxacin hydrochloride by photo-Fenton oxidation process, *Environmental Engineering Science*, **26**(4), 753–759.

Sun W., Chu H., Dong B., Cao D., Zheng S. (2014), The degradation of naproxen and diclofenac by a nano-TiO_2/diatomite photocatalytic reactor, *International Journal of Electrochemical Science,* **9***,*4566–4573.

Swamy G.J., Sangamithra A. and Chandrasekar V. (2014), Response surface modeling and process optimization of aqueous extraction of natural pigments from Beta vulgaris using Box–Behnken design of experiments, *Dyes and Pigments,* **111**, 64–74.

Tamaddon F., Mosslemin M.H., Asadipour A., Gharaghani M.A. and Nasiri A. (2020a). Microwave-assisted preparation of $ZnFe_2O_4$@methyl cellulose as a new nano-biomagnetic photocatalyst for photodegradation of metronidazole, *International Journal of Biological Macromolecules,* **154**, 1036–1049.

Tamaddon F., Nasiri A. and Yazdanpanah G. (2020b). Photocatalytic degradation of ciprofloxacin using

$CuFe_2O_4$@methyl cellulose based magnetic nanobiocomposite, *MethodsX,* **7**, 74–81.

Torki F. and Faghihian H. (2018), Visible Light Degradation of Naproxen by Enhanced Photocatalytic Activity of NiO and NiS, Scavenger Study and Focus on Catalyst Support and Magnetization, *Photochemistry and Photobiology,* **94**(3), 491–502.

Turki A., Guillard C., Dappozze F., Ksibi Z., Berhault G. and Kochkar H. (2015), Phenol photocatalytic degradation over anisotropic TiO_2 nanomaterials: Kinetic study, adsorption isotherms and formal mechanisms, *Applied Catalysis B: Environmental,* **163**,404–414.

Wang Y., Shi R., Lin J. and Zhu Y. (2011), Enhancement of photocurrent and photocatalytic activity of ZnO hybridized with graphite-like C_3N_4. *Energy & Environmental Science*, **4**(8), 2922–2929.

Yao H., Li F., Lutkenhaus J., Kotaki M. and Sue H.J. (2016). High-performance photocatalyst based on nanosized ZnO-reduced graphene oxide hybrid for removal of Rhodamine B under visible light irradiation, *AIMS Materials Science*, **3**, 1410–1425.

Zhang L., Cheng H., Zong R. and Zhu Y. (2009), Photocorrosion suppression of ZnO nanoparticles via hybridization with graphite-like carbon and enhanced photocatalytic activity, The Journal of Physical Chemistry C, **113**(6), 2368–2374.

Zhang H., Zhang P., Ji Y., Tian J. and Du Z. (2015), Photocatalytic degradation of four non-steroidal anti-inflammatory drugs in water under visible light by P25-TiO_2/tetraethyl orthosilicate film and determination via ultra performance liquid chromatography electrospray tandem mass spectrometry, *Chemical Engineering Journal,* **262**, 1108–1115.

Zheng S., Jiang W., Cai Y., Dionysiou D.D. and O'Shea K.E. (2014), Adsorption and photocatalytic degradation of aromatic organoarsenic compounds in TiO_2 suspension, *Catalysis Today,* **224**, 83–88.